JOURNAL OF NEUROPHYSIOLOGY
Vol. 68, No. 1, July 1992. *Printed in U.S.A.*

Effect of Stimulus Contrast and Size on NMDA Receptor Activity in Cat Lateral Geniculate Nucleus

YOUNG H. KWON, SACHA B. NELSON, LOUIS J. TOTH, AND MRIGANKA SUR
Department of Brain and Cognitive Sciences, Massachusetts Institute of Technology, Cambridge, Massachusetts 02139

SUMMARY AND CONCLUSIONS

1. We studied the effect of varying excitatory and inhibitory drive on the *N*-methyl-D-aspartate (NMDA) receptor–mediated component of the visual responses of neurons in the cat dorsal lateral geniculate nucleus (dLGN) by varying the contrast and size of stimuli presented to the receptive fields of these cells.

2. Cells were classified as either on- or off-center, X or Y, and lagged or nonlagged. Stimulus contrast, and hence the amount of excitatory drive, was varied by changing the brightness of a spot, whose size and location matched the cell's receptive field center, relative to a fixed background luminance. Responses to varying contrast were collected from each cell before, during, and after iontophoretic application of D-2-amino-5-phosphonovaleric acid (D-APV), a specific NMDA receptor antagonist. From each contrast-response plot, a sigmoidal curve fit yielded five parameters on which we examined the effect of D-APV: the threshold contrast, saturation contrast, contrast at half saturation (C_{50}), slope (gain) at C_{50}, and saturation response.

3. In most cells, application of D-APV reduced both the saturation response and the gain of the contrast-response curve, but did not reduce or change significantly the threshold contrast, saturation contrast, or C_{50}.

4. Cells varied in their sensitivity to D-APV, but for any given cell, the D-APV–sensitive component was nearly always a linear function of the control visual response level. Thus, for a spot of optimal size, there was a constant proportion of the visual response attributable to NMDA receptors, regardless of the amplitude of the response.

5. When the effect of D-APV on the visual responses to an optimal spot at varying contrasts was compared among different classes of dLGN cells, the visual responses of lagged X cells were reduced to a greater extent than those of either nonlagged X cells or the combined population of nonlagged X and Y cells.

6. Stimulus size (spot diameter) was also varied systematically at a fixed contrast to vary the inhibitory drive to dLGN cells. As stimulus size was increased, the response first increased because of increased stimulation of the receptive field center and then decreased because of increasing amounts of surround inhibition.

7. The D-APV–sensitive component of individual cell responses was greater when the stimulus spot was less than or equal to optimal size than when the spot was larger. Thus the contribution of NMDA receptors to the visual response decreased with increasing surround inhibition.

8. These results show that the fraction of the visual response of a dLGN cell mediated by NMDA receptors is not modulated by the amount of retinal excitatory drive. Rather, the proportional contribution of NMDA receptors to the visual response remains constant over the entire range of stimulus contrasts used. The results also suggest that the relative contribution of NMDA receptors may be decreased by lateral inhibition in the dLGN. Thus modulation of NMDA receptor activation on dLGN cells during visual transmission appears to be a dynamic, ongoing process subject to the specific spatial distribution of excitation and inhibition on dLGN cells.

INTRODUCTION

Excitatory amino acid (EAA) receptors mediate synaptic transmission in many areas of the vertebrate CNS (for reviews, see Cotman et al. 1987; Mayer and Westbrook 1987). These receptors can be broadly categorized into two groups: the *N*-methyl-D-aspartate (NMDA) receptors and the non-NMDA receptors. The latter group includes quisqualate and kainate receptors, which may or may not comprise separate classes. The two types of EAA receptors differ not only in their responses to various agonists but also in their ionic selectivities and voltage dependence. Non-NMDA receptors conduct primarily monovalent Na^+/K^+ ions when activated (MacDermott and Dale 1987; see, however, Gilbertson et al. 1991), whereas NMDA receptors also conduct Ca^{2+}, an important divalent cation. In addition, the NMDA receptor channel, unlike most other ligand-gated channels, is voltage dependent; at hyperpolarized, but not depolarized, potentials, it is blocked by physiological levels of Mg^{2+} ions (Mayer and Westbrook 1987).

There is growing evidence that NMDA receptors are involved in normal sensory transmission in the brain. A number of in vivo and in vitro studies have now documented that both types of EAA receptors contribute to retinogeniculate transmission (Crunelli et al. 1987; Esguerra et al. 1992; Funke et al. 1991; Hartveit and Heggelund 1990; Heggelund and Hartveit 1990; Kemp and Sillito 1982; Kwon et al. 1991; Scharfman et al. 1990; Sillito et al. 1990a,b). Given the unique properties of the NMDA receptor, an important goal of pharmacological studies of retinogeniculate transmission is to characterize similarities and differences in the responses of dorsal lateral geniculate nucleus (dLGN) cells mediated by the two types of EAA receptor. Iontophoretic studies in the cat dLGN have shown that both receptors mediate visual responses in each of the major classes of relay cells (on- and off-center or X and Y). Although individual cells vary widely in their sensitivities to blockade of NMDA and non-NMDA receptors, no consistent differences in the role of the two receptor types are observed between these dLGN cell classes (Kwon et al. 1991; Sillito et al. 1990a,b).

Recently, relay neurons in the cat dLGN have also been classified with respect to the temporal properties of their responses to stimuli turning on or off within their receptive fields (Humphrey and Weller 1988a; Mastronarde 1987a,b,

1988; Saul and Humphrey 1990). Nonlagged cells respond to such stimuli with a time course that is similar to that of retinal ganglion cell responses. Their responses are characterized by transient discharge at short latency after stimulus onset. In contrast, lagged cells have a long visual latency to a flashing stimulus and lack the initial onset transient burst of discharge. Most lagged cells also have an offset discharge that decays slowly to background levels. Lagged X cells have tonic or sustained responses to maintained stimuli. Lagged and nonlagged cells may represent unique dLGN cell classes (Humphrey and Weller 1988b), or different response modes of the same neuron (Uhlrich et al. 1990). Iontophoretic studies in vivo have shown that although both types of cell are susceptible to NMDA and non-NMDA receptor blockade, the visual responses of lagged cells are affected more by NMDA receptor antagonists than those of nonlagged cells (Heggelund and Hartveit 1990; Kwon et al. 1991).

A motivation for the present study was to examine the differences in sensitivity to NMDA receptor blockade that we and others have observed both within and across relay cell classes. Given the voltage dependence of the NMDA response in the LGN in vitro (Esguerra et al. 1992), we wished to test the hypothesis that differences in sensitivity to NMDA receptor blockade reflect differences in the balance of excitation and inhibition evoked by visual stimulation. In a previous study, we found that the difference between lagged and nonlagged cells in the sensitivity to NMDA receptor blockade was not correlated with the visual activity levels of the two populations (Kwon et al. 1991). Comparisons across cells may, however, be complicated by technical difficulties of iontophoretic experiments. It is difficult to know, for example, whether differences between cells reflect different cellular properties or variations in the efficacy of antagonism. In the present study, we have examined this issue more carefully by studying the NMDA receptor contribution to individual cell responses while presenting a range of different visual stimuli. By varying the contrast of a small spot, we varied the amount of excitatory drive to the cell (see also Fox et al. 1990). By varying the size of the spot, we varied the amount of inhibitory drive to the cell through surround inhibition (Hubel and Wiesel 1961).

Our results show that the fraction of the visual response mediated by NMDA receptors remains the same when the excitatory drive to dLGN cells is varied by varying stimulus contrast. Thus the NMDA receptor component at low visual response levels is proportionately the same as at high response levels. However, the contribution of NMDA receptors becomes proportionately smaller as the amount of inhibitory input is increased by increasing the stimulus size.

METHODS

Animal preparation

Experiments were performed on adult cats that were prepared for extracellular electrophysiological recording as described previously (Kwon et al. 1991; Sur et al. 1987). Briefly, animals were anesthetized (induction and surgery with 3% halothane in 70% N_2O-30% O_2; maintenance with 0.6–1% halothane), paralyzed (3.6 mg/hr gallamine triethiodide and 0.7 mg/hr *d*-tubocurarine), and artificially ventilated. End-tidal CO_2 was maintained at 4% and body temperature at 38°C. An electrocardiogram was continuously monitored to maintain the heart rate at the pre-paralysis level by appropriately adjusting the halothane dose. Pupils were dilated and a set of contact lenses were fitted to focus the eyes on an oscilloscope screen 57 cm in front of the animal. The precision of focus was insured by the use of an ophthalmic retinoscope as well as by reflecting an image of the retinal surface onto a tangent screen. A pair of bipolar stimulating electrodes was placed across the optic chiasm. A craniotomy (1–2 cm diam) was made to expose the cortex overlying the dLGN.

Microiontophoresis

A six-barreled glass micropipette electrode assembly was used for extracellular recording as well as for iontophoretic application of various drugs (Kwon et al. 1991). The recording micropipette was filled with 3 M KCl, and each of the other pipettes was filled with one of the following solutions (in H_2O): NMDA (50 mM, pH 8.0), kainic acid (KA; 20 mM, pH 8.0), D-2-amino-5-phosphonovaleric acid D-APV; 50 mM, pH 8.0, and 6-cyano-7-nitroquinoxaline-2,3-dione (CNQX; 12.5 mM, pH 9.8). A barrel filled with 150 mM NaCl was used as a balance barrel and in a few cases was used to assess direct effects of iontophoretic current.

Antagonists were applied at doses found to be adequate yet specific with respect to responses to applied agonists. This was achieved by carefully titrating the antagonist dose until it completely blocked the appropriate agonist response (NMDA for the antagonist D-APV and KA for the antagonist CNQX), but not responses to other agonists (see Kwon et al. 1991 for details). Visual responses at various spot contrasts and sizes were collected before, during, and after application of each antagonist.

Cell classification

The receptive field of each cell was plotted on a tangent screen and was classified as either on- or off-center and X or Y. The latter classification was based on the receptive field size at a given eccentricity, latency to optic chiasm stimulation, and linearity of spatial summation determined with a counterphasing grating (Shapley and Lennie 1985; Sherman and Spear 1982; Sur et al. 1987). Cells were also divided into lagged and nonlagged types on the basis of their visual latencies at onset of a spot of the appropriate contrast (Hartveit and Heggelund 1990; Heggelund and Hartveit 1990; Humphrey and Weller 1988a; Mastronarde 1987a, 1988; Saul and Humphrey 1990; see Kwon et al. 1991 for specific criteria). Lagged cells had start-rise and half-rise visual latencies >45 and 55 ms, respectively; those of nonlagged cells were smaller than these values.

Visual stimulus

The stimulus was produced with a Picasso stimulus generator (Innisfree, Cambridge, MA) under microcomputer (IBM compatible PC) control and presented on a Tektronix 620 monitor. The visual stimulus consisted of a spot whose luminance varied from darker than background to brighter than background. Contrast was calculated as (center luminance − background luminance)/(center luminance + background luminance). In the case of on-center cells, for example, negative contrast consisted of spots darker than background and positive contrast, the spots brighter than background. In one set of experiments, spot contrast was modulated from light to dark at 2 Hz and spot size was matched to the receptive field center size. To minimize the effect of any systematic changes in response during the test period, 12–24 different contrast levels were interleaved in a random order for a given cell, and each contrast level was presented a total of 10 times. Back-

ground screen luminance was 5.87 cd/m^2 and represented the zero contrast level; the response at zero contrast was taken to be the background firing level. (In later experiments, mean luminance was varied between 2 values, 3.00 and 8.14 cd/m^2, for on- and off-center cells, respectively, to obtain a greater positive range of contrasts). Maximal ranges of contrasts obtained this way were between −0.85 and 0.73 for on-center cells and between −0.4 and 0.95 for off-center cells. In a second set of experiments, stimulus spot size was systematically varied between 0.5, 1, 2, 4, and 8 times the cell's receptive field center size; spots were presented randomly, and each size was presented 10 times. Stimulus contrast was kept constant for a given cell and ranged between 0.5 and 0.72 for on-center cells and between 0.85 and 0.95 for off-center cells. All responses were collected on-line and stored in the microcomputer as well as on videotape, with the use of a data encoder, for off-line analysis (Neurocorder DR-886, Neuro Data Instruments, New York, NY).

Data analysis

Averaged peristimulus time histograms (PSTHs) were constructed from the 10 trials for each spot contrast and size obtained before, during, and after antagonist application. Mean firing rate over the entire response period (500 ms) as well as peak firing rate (using a 100-ms moving average window) was computed and plotted as a function of spot contrast and size.

Contrast-response plots were constructed by plotting mean firing rate against stimulus contrast. The plot was fitted with an expression of the form

$$R = R_s \times C^n/(C^n + C_{50}{}^n) + R_m,$$

where R is response, C is contrast, R_s is saturation response, R_m is minimum response, C_{50} is contrast at half saturation response, and n is measure of steepness of the linear portion. The function, when plotted, is of a sigmoidal shape. Thus the curve fit assumes that the response has a stable minimum and a maximum (saturation) and a linear range between the two. R_s, R_m, and C_{50} are directly determined by the curve fit. The slope at C_{50} can be derived by differentiating the expression and evaluating R at C_{50}. We defined the threshold and saturation contrasts as the points on the abscissa where the line crossing the C_{50} point with the slope calculated as above crosses the minimum and maximum responses, respectively. The five parameters from the contrast-response function that we used to examine the effect of D-APV were the threshold contrast, saturation contrast, C_{50}, slope at C_{50}, and R_s (see Fig. 1). Note that the threshold and saturation contrasts define the linear range and the slope defines the gain of the function.

To determine whether or not the NMDA receptor–mediated component of the response remains constant with response level, we plotted the D-APV–sensitive component of the visual response as a function of the control response amplitude (that is, before the application of antagonist). The D-APV–sensitive component was calculated by subtracting the response obtained during D-APV application from the control response. A linear plot would indicate that NMDA receptors contribute a constant fraction of the overall response, with the fraction determined by the slope of the line (see below). The D-APV–sensitive fractions were compared between different cell classes with the use of an unpaired nonparametric statistical test (Mann-Whitney U test).

The responses to different-sized spots were divided into two groups. The (receptive field) "center" responses comprised those responses collected at sizes equal to or smaller than the optimal size; the "center + surround" responses comprised responses collected at sizes greater than the optimal spot size. The optimal size was defined as the stimulus size at which the cell's response was the greatest, therefore representing the size closest to the receptive field center size. The D-APV–sensitive fractions of the center and center + surround responses were compared with each other as well as with the D-APV–sensitive fractions obtained from the contrast study with the use of a paired nonparametric test (Wilcoxon signed-rank test).

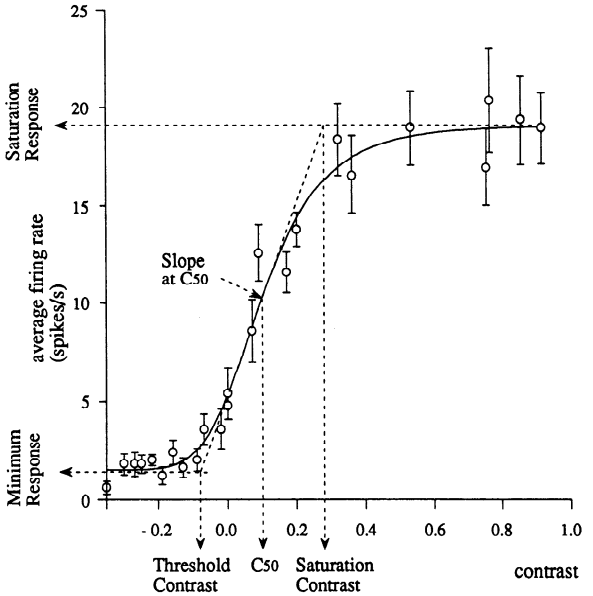

FIG. 1. Contrast-response curve of an off-center nonlagged X cell. Positive contrast values refer to dark spots and negative contrast to bright spots, relative to a fixed background luminance of 5.87 cd/m^2; zero contrast refers to an uniform illumination of the visual field. Average firing rate is computed over 0.5 s, which was the period of stimulus presentation. Error bars: SE of 10 trials. The contrast-response curve is sigmoidal in shape, and a curve fit was performed as described in METHODS (r = 0.990).

RESULTS

We report on a total of 39 cells recorded from the A laminae of the dLGN, including 24 X cells and 15 Y cells. The X cells included 20 nonlagged cells and 4 lagged cells. All the Y cells were nonlagged; we recorded no lagged Y cells in the present study. Our criteria for classifying cells as X or Y and as lagged or nonlagged have been described in detail previously (Kwon et al. 1991), and these criteria were adhered to strictly in the present study. Of the total, 38 cells were tested with varying stimulus contrast (19 nonlagged X cells, 4 lagged X cells, and 15 nonlagged Y cells) and 34 cells were tested with varying stimulus size (20 nonlagged X cells, 1 lagged X cell, and 13 nonlagged Y cells).

Effect of D-APV on responses to spots of varying contrasts

Figure 1 shows the effect of contrast on the visual response of an off-center nonlagged X cell. The cell's response approximates a sigmoidal shape, with a minimum and saturation response and linear range in between. Positive contrasts indicate spots darker than background luminance, and negative contrasts indicate brighter spots (see METHODS). At zero contrast (no visible spot, background mean luminance of 5.87 cd/m^2) there was still a fair amount of response, and only for negative contrast values did the cell's response reach a sustained minimum. We always presented spots with both negative and positive contrasts to ensure a full range of visual responses. A sigmoidal curve fit yielded the parameters that are useful for characterizing the func-

tion (see METHODS). The linear contrast range for this cell was −0.08 to 0.28; C_{50} was 0.10. The slope at C_{50} was 49.09 ($r = 0.990$), and the saturation response was 19.14 spikes/s. The slope provides a measure of the gain with which the input (contrast) is encoded into firing rate. The contrast-response plots of most cells were similar to the one shown in Fig. 1 (see Figs. 2, 3, and 5).

Figure 2*A* shows the contrast-response curve from the same cell before, during, and after 60 nA of D-APV application. The levels of D-APV ejection current used in the study were carefully adjusted to block NMDA receptor responses without affecting responses to applied kainate and were generally between 60 and 90 nA (METHODS; see also Kwon et al. 1991). The contrast-response curve obtained during D-APV application was similar in its overall shape to that obtained before drug ejection. There was no significant change in the threshold or saturation contrasts. The slope at C_{50}, however, decreased significantly from 49.09 to 21.67 (a reduction of 56%), and the saturation response decreased from 19.14 to 11.38 spikes/s. Thus the blockade of NMDA receptors appeared to have significantly decreased the contrast gain and saturation response while having only limited influence on the threshold contrast, saturation contrast, and C_{50}. Conversely, the contribution of NMDA receptors was to increase the gain and saturation response of the contrast-response curve without significantly changing the contrasts at which the response reached threshold or saturation. That is, the function of NMDA receptors was to amplify the visual signal in the linear range of the response.

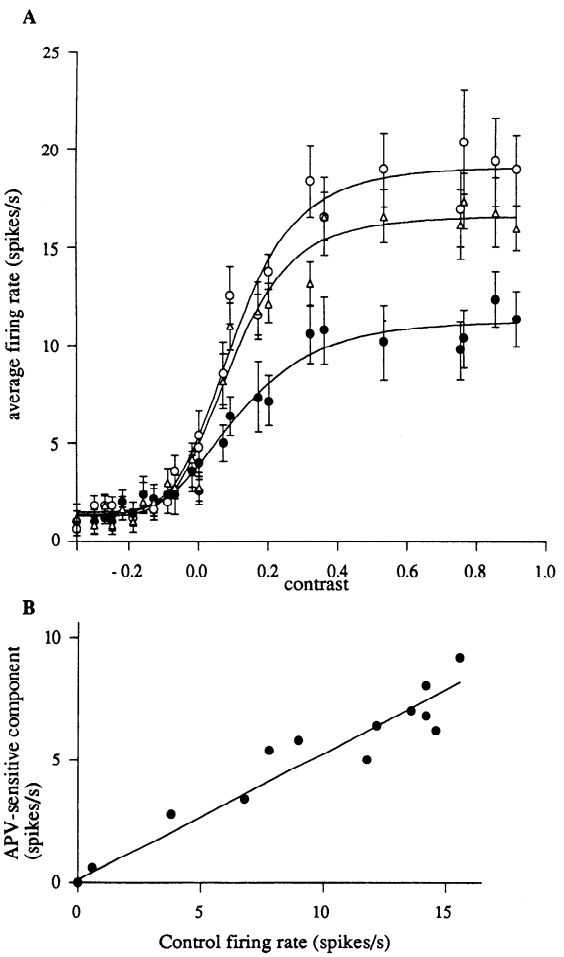

FIG. 2. Effect of D-2-amino-5-phosphonovaleric acid (D-APV) on the contrast-response plot of the cell in Fig. 1. *A*: contrast-response plot before (○), during (●), and 2 min after (△) 60 nA of D-APV application. Conventions as in Fig. 1. *B*: D-APV sensitive component is calculated by subtracting the responses during D-APV application from those before application. The line represents the least-squares fit with a slope of 0.515 ($r = 0.982$). The D-APV–sensitive component was approximately linear function of the control visual response level.

Sigmoidal curves were fitted to the contrast-response curves of all 38 cells. A subset of 25 cells (13 nonlagged X and 12 nonlagged Y) that yielded a reasonably good fit ($r \geq 0.80$; mean $r = 0.95$) was chosen for population analysis. [In 9 of the remaining 13 cells, curve fits to the sigmoidal function were not appropriate; visual responses of the 9 cells (4 nonlagged X, 4 lagged X, and 1 nonlagged Y) were so severely reduced by D-APV application (86.1 ± 4.7% reduction) that sigmoidal curve fits of responses obtained during D-APV application produced threshold and saturation contrasts that were rather arbitrary. Four of these 13 cells generally produced poor fits to the sigmoidal function. In these cells, the variation in data points was likely due to several sources, including fluctuations in the "background" firing level of the cells. Importantly, all 4 cells had their saturation responses severely affected by D-APV]. Table 1 compares five relevant parameters of the contrast-response curve before and after D-APV application. Consistent with the results obtained from the cell shown in Fig. 2*A*, the population parameters show little change in the threshold contrast, saturation contrast, and C_{50} during D-APV application ($P > 0.2$ for all 3 parameters, Wilcoxon signed-rank test). Of the 25 cells pooled, 1 cell showed a significant change in threshold contrast with D-APV application, whereas 5 cells showed a significant change in the saturation contrast. The slope at C_{50} and the saturation response, however, showed significant decreases with D-APV ($P < 0.001$ for both parameters, Wilcoxon signed-rank test).

In Fig. 2*B*, the D-APV–sensitive component of the visual response (as calculated by subtracting the response during D-APV application from the control response) is plotted as a function of the magnitude of the control visual response (visual response minus background activity). The relationship is linear, implying that the D-APV–sensitive component remained proportionally the same throughout the entire range of visual response. The points are well fitted by a line of slope 0.52 ($r = 0.982$), indicating that 52% of the visual response at any contrast was due to NMDA receptors and was therefore sensitive to NMDA receptor blockade. This value (which will be referred to as the "D-APV–sensitive fraction" hereafter) also corresponds closely to the change in the gain of the contrast-response curve in Fig. 2*A*.

This linear relationship was quite consistent from cell to cell. Figure 3*A* shows the contrast-response curves of another off-center nonlagged X cell before, during, and after 86 nA of D-APV application. The slope decreased significantly, from 52.32 to 19.56 (a reduction of 62.6%). Figure 3*B* shows that the same cell's D-APV–sensitive component is again a linear function of the visual response, with a slope of 0.75 ($r = 0.996$). Figure 3*C* shows contrast-response curves from an on-center nonlagged Y cell. The visual response did not reach saturation up to a stimulus contrast of

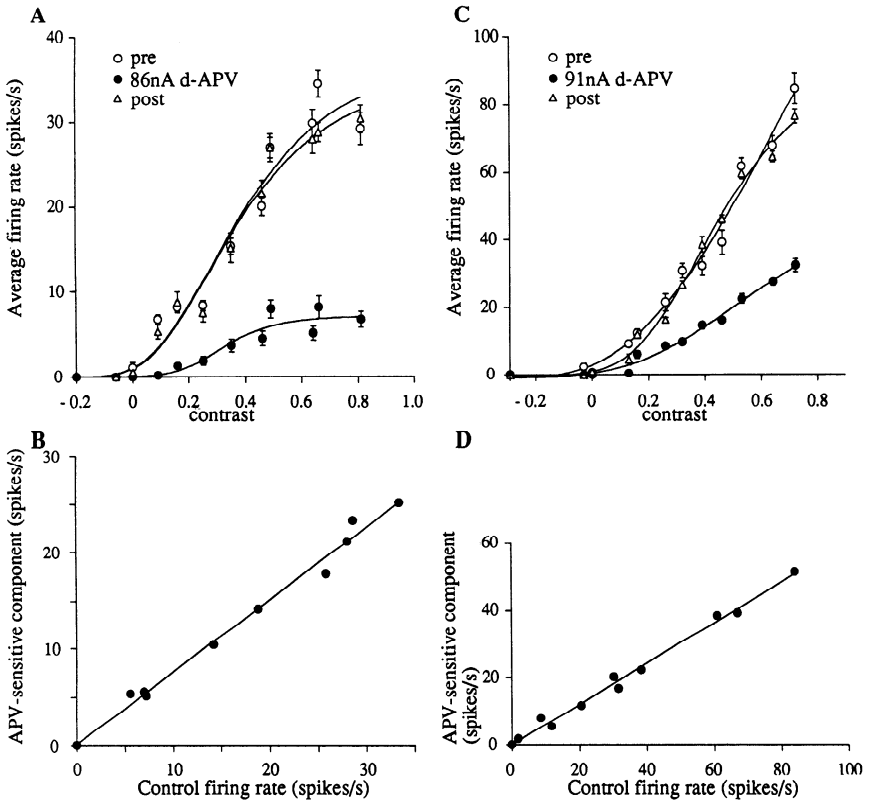

FIG. 3. Effect of D-2-amino-5-phosphonovaleric acid (D-APV) on the contrast-response plots of 2 cells with different D-APV-sensitive fractions in their visual responses. Conventions as in Fig. 2. *A*: contrast-response plots of an off-center nonlagged X cell before, during, and after 86 nA of D-APV application. *B*: same cell as in *A*. The best linear fit has a slope of 0.753 (r = 0.996). *C*: contrast-response plots of an on-center nonlagged Y cell before, during, and 1.5 min after 91 nA of D-APV application. *D*: same cell as in *C*. The line of best fit has a slope of 0.604 (r = 0.996). There is a linear relationship between the D-APV-sensitive component and the control visual response level in both cells even at different absolute values of the slopes.

0.7. Nevertheless, it is evident that D-APV affected the gain of the linear portion of the curve, which decreased from 152.37 to 52.93. Figure 3*D* shows that the D-APV-sensitive component was a linear function of the cell's control response, with a slope of 0.60 (r = 0.996). Importantly, the three cells illustrated in Figs. 2 and 3 all showed a linear relationship between the D-APV-sensitive component and the amplitude of the control visual response, despite different absolute values of the D-APV-sensitive fractions (Figs. 2*B* and 3, *B* and *D*).

Representative PSTHs for the off-center, nonlagged X cell of Fig. 3, *A* and *B*, are shown in Fig. 4. The increase in the cell's response with contrast consisted of an increase in both the onset transient and the sustained components of response (Fig. 4, *A–C*). D-APV substantially decreased the response at all contrasts, including the transient and sustained components. We did not observe any consistent differences in the effects of APV on transient (e.g., Fig. 4) and sustained (e.g., Fig. 9) responses. Both types of responses were well represented in our population. Roughly two thirds of the cells studied (26 of 38) had responses which, like those shown in Fig. 4, contained a transient component (defined as the response between 0- and 100-ms latency) that was more than twice the magnitude of the sustained component (defined as the response between 200- and 500-ms latency). The remaining cells, like the one shown in Fig. 9, showed more prominent sustained responses.

The linear relationship between the D-APV-sensitive component and control visual response was observed in all physiological classes of cells that we recorded. Figure 5*A* shows an on-center nonlagged X cell for which the slope of the D-APV-sensitive component versus control response line (the D-APV-sensitive fraction) was 0.75 (r = 0.99). Figure 5*B* shows an off-center lagged X cell in which the D-APV-sensitive fraction of the visual response was also 1.00 (r = 1.000). That is, the visual response of this lagged X cell was completely abolished with the application of D-APV. All four lagged X cells that we recorded showed linear relationships and high values of the D-APV-sensitive fraction of their visual responses (see below). Figure 5*C* shows an on-center nonlagged Y cell in which the D-APV fraction was 0.58 (r = 0.98). A linear plot of the D-APV-sensitive

TABLE 1. *Parameters of the contrast-response function and the effect of D-APV*

	Control	D-APV	APV—Control
Threshold contrast	0.017 ± 0.021	0.019 ± 0.028	0.001 ± 0.024 (0.84)
Saturation contrast	0.398 ± .047	0.367 ± 0.062	−0.031 ± 0.05 (0.57)
Contrast at C_{50}	0.208 ± 0.027	0.193 ± 0.041	−0.015 ± 0.024 (0.25)
Slope at C_{50}	174.103 ± 26.408	75.924 ± 14.893	−98.179 ± 24.241 (0.0005)
Saturation response, spikes/s	51.49 ± 5.91	24.546 ± 4.49	−26.945 ± 5.814 (0.0001)

Values are means ± SE; n = 25. Numbers in parentheses are P values. Statistical comparisons employed the Wilcoxon signed-rank test. The only two parameters of the contrast-response curve that significantly changed with D-APV application were C_{50} and saturation response; other parameters did not change significantly. D-APV, D-2-amino-5-phosphonovaleric acid; C_{50}, half saturation contrast.

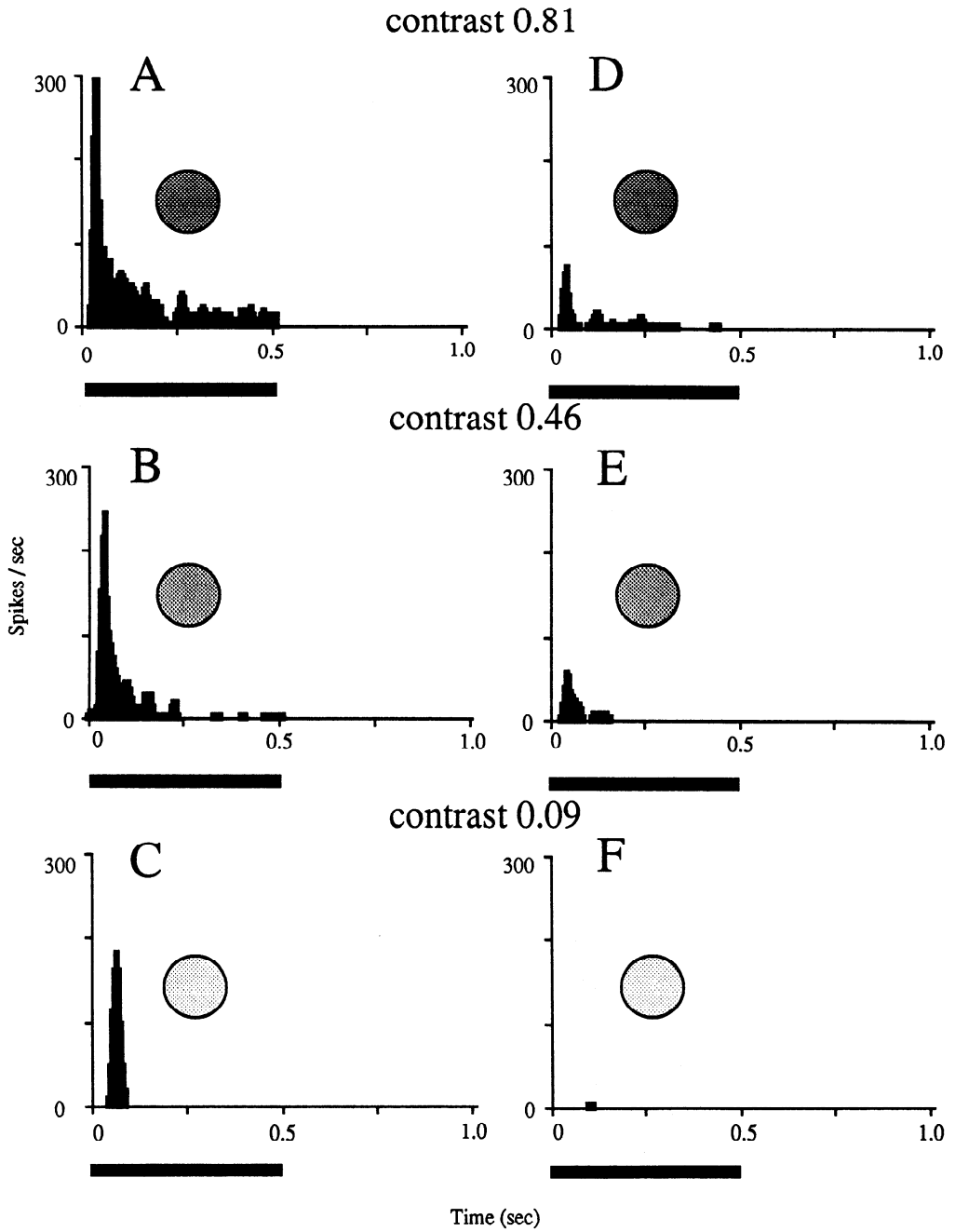

FIG. 4. Responses of an off-center X cell to spots at 3 different contrast and the effect of D-2-amino-5-phosphonovaleric acid (D-APV). The contrast-response curves of this cell are shown in Fig. 3*A*. Each peristimulus time histogram represents the summed response to 10 presentations of a dark spot matched in size to the receptive field center. Each bin spans 5 ms. Timing and duration of the visual stimulus is indicated by the bar below each histogram. *A–C*: control (pre-drug) responses at indicated contrasts. *D–F*: responses at same contrasts during iontophoretic application of D-APV (86 nA). Note the substantial reduction of the response at all contrasts.

component as a function of the control response was found in most of the cells that we tested; 27 of the 38 cells we tested could be fit with a straight line with correlation coefficient (r) greater than 0.9. Of the remaining 11, 2 could be fit with $r > 0.8$ and 1 with $r > 0.7$. The mean correlation coefficient (r) for the entire population was 0.837 ± 0.044 ($n = 38$).

Figure 6 shows two cells that did not show linear relationships between the D-APV–sensitive component and the control visual response. Figure 6*A* shows contrast-response curves from an off-center nonlagged X cell. As in the previous examples, the sigmoidal shape of the curve was retained during the D-APV application. The gain of the curve decreased from 102.66 to 44.53 while the saturation response decreased from 30.25 to 12.72 with D-APV. The plot of the D-APV–sensitive component against the control response showed a slight nonlinearity (Fig. 6*B*). This was the only cell that showed an increase in the D-APV–sensitive fraction with increasing control responses, consistent with a slight voltage dependence of the NMDA component at postthreshold membrane potentials. Figure 6*C* shows contrast-response curves from another off-center non-

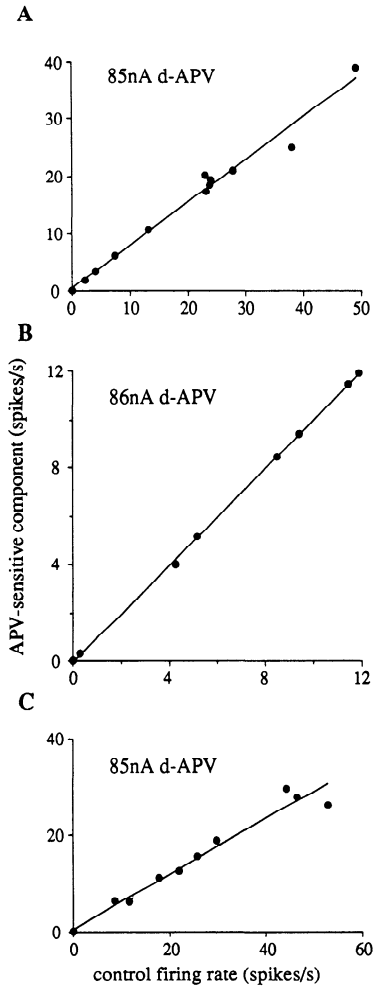

FIG. 5. Plots of the D-2-amino-5-phosphonovaleric acid (D-APV)-sensitive component as a function of the control level of response in different dorsal lateral geniculate nucleus (dLGN) cell classes. There is a constant contribution from *N*-methyl-D-aspartate (NMDA) receptors to the visual responses of all 3 cells. *A*: on-center nonlagged X cell with 85 nA of D-APV application. Slope = 0.748 (r = 0.99). *B*: off-center lagged X cell with 86 nA of D-APV application. Slope = 1.002 (r = 1.0). *C*: on-center nonlagged Y cell with 85 nA of D-APV application. Slope = 0.576 (r = 0.98).

lagged X cell. Application of 83 nA of D-APV seemed to reduce the visual responses by a constant amount (except at the highest contrast), and the gain of the curve changed very little. The linear range of contrast decreased significantly from −0.13/0.72 to 0.17/0.47, but the C_{50} changed little from 0.29 to 0.32. The slope actually increased from 78.42 to 97.39 with D-APV. Figure 6*D* shows that the cell's D-APV-sensitive component is a highly nonlinear function; however, for the most part, the function is roughly constant (with a value near 14). The plot indicates that the absolute contribution of NMDA receptors to the visual response was approximately constant at all levels of response. A similar result has been reported in deeper layers of the cat visual cortex (see Fig. 4*D* of Fox et al. 1990). In general, however, these nonlinear effects of D-APV were not common in the dLGN (observed in 8 of 38 cells); most cells showed a linear relationship between the D-APV-sensitive component and control visual response level, with a slope between 0 and 1.

Proportion of the visual response mediated by NMDA receptors in different cell classes

The D-APV-sensitive proportions obtained by varying stimulus contrast can be used to compare the NMDA receptor-mediated fractions of visual responses among different cell classes. Figure 7 shows the frequency distribution histogram of the D-APV-sensitive proportions in the three different cell types we recorded. The lagged X cells as a group had the greatest proportion of their visual responses mediated by NMDA receptors (mean of 0.896 ± 0.065, n = 4). The nonlagged X cells were next, with a mean proportion of 0.636 ± 0.070 (n = 19), whereas the nonlagged Y cells had a mean of 0.567 ± 0.100 (n = 15). The difference between lagged X and nonlagged Y cells was statistically significant ($P < 0.04$, Mann-Whitney U test), as was the difference between lagged X cells and the combined population of nonlagged X and Y cells ($P < 0.04$, Mann-Whitney U test).

Simultaneous blockade of NMDA and non-NMDA receptors

In a few cells (n = 3), we also applied CNQX, a specific non-NMDA receptor antagonist, to see whether the remaining visual response in the presence of D-APV, the NMDA receptor antagonist, is mediated by non-NMDA receptors. Figure 8 shows the contrast-responses curves of an off-center nonlagged X cell (the same cell as in Fig. 6*A*). Application of D-APV significantly decreased the visual response; simultaneous application of D-APV and CNQX completely abolished the visual response, indicating that all of the visual response of this neuron was mediated by EAA receptors.

Effect of D-APV on responses to spots of varying sizes

Increasing the size of a stimulus spot first caused lateral geniculate nucleus (LGN) cell responses to increase as the spot covered more of the receptive field center and then to decrease as the spot increasingly encroached on the surround. Figure 9 shows PSTHs from an off-center, nonlagged X cell responding to a spot matched to the receptive field center (1 deg diam) and to a spot four times the diameter (Fig. 9, *A* and *B*). The larger spot caused a reduction in all components of the response, including early transient and late sustained components. Iontophoresing D-APV caused a significant reduction in the response to the 1-deg spot (Fig. 9*C*) but had little effect on the 4-deg spot (Fig. 9*D*). The proportion of the cell's visual response mediated by NMDA receptors thus differed remarkably depending on spot size, and hence on the extent to which surround inhibition was engaged by the stimulus.

We have evaluated quantitatively the change in LGN cell responses with spot size as well as the effect of D-APV on these responses. Figure 10 shows the visual responses of an off-center nonlagged X cell to a spot of increasing size (at a fixed contrast of 0.92). Peak firing rates with a 100-ms moving average window are shown because they showed slightly greater depth of modulation with changes in stimulus size than average firing rates over a 500-ms response period. Both measures, however, yielded the same qualita-

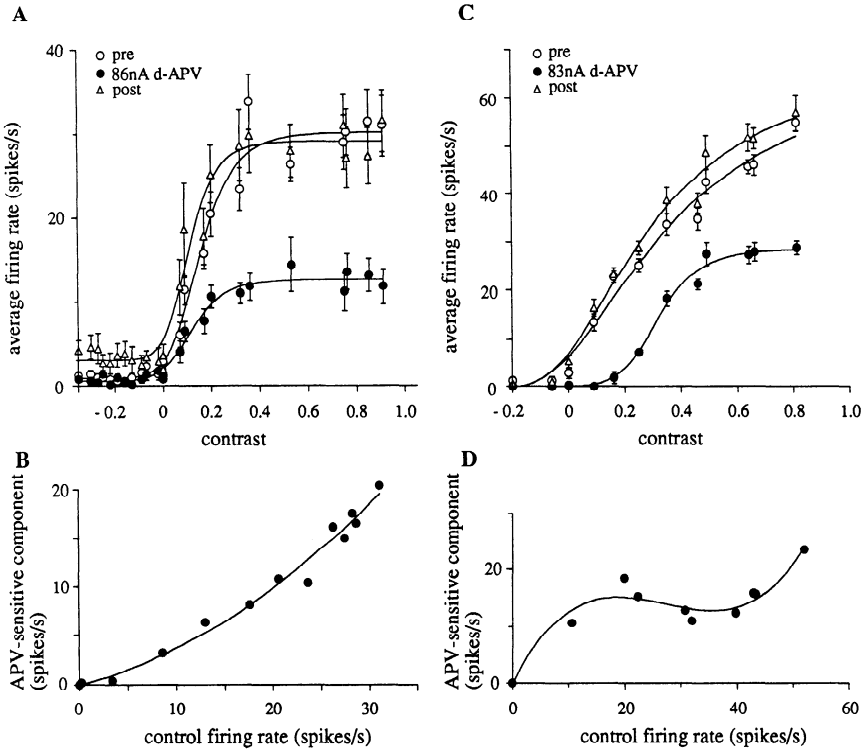

FIG. 6. Contrast-response curves of 2 X cells in which the plots of the D-2-amino-5-phosphonovaleric acid (D-APV)-sensitive component as a function of the control visual response deviated from linearity. Conventions as in Fig. 2. *A*: off-center nonlagged X cell before, during 86 nA of D-APV iontophoresis, and 2 min after iontophoresis. *B*: same cell as in *A*. The curve is a second order polynomial fit. *C*: another off-center nonlagged X cell before, during, and 5 min, 20 s after 83 nA of D-APV application. *D*: same cell as in *C*. The curve is a 3rd-order polynomial fit.

tive results. The cell's response increased as the spot diameter increased from 0 (no spot) to 1.2–2.4 deg (the optimal size). As the size increased further to 4.8 and 9.6 deg, the response decreased as a result of increasing surround inhibition (because of both retinal and geniculate mechanisms). It is apparent that two different spot sizes can produce the same magnitude of response. For example, in Fig. 10, the response are similar at spot diameters of 1.2 and 9.6 deg (62.0 and 64.0 spikes/s at 1.2 and 9.6 deg, respectively). However, the mechanism by which this submaximal response is achieved differs for the two spot sizes: the small spot does not provide enough excitatory drive, whereas the large spot likely engages intraretinal inhibition (causing some reduction in retinal excitatory drive) as well as increased lateral intrageniculate inhibition (Sillito and Kemp 1983; see also below). Despite the similar response levels, the effect of D-APV was dramatically different for the large spot compared to the small one (see below). To facilitate comparison, we divided these responses into two groups: center responses, which included responses to spots equal to or smaller than the optimal size, and center + surround responses, which included responses to spots greater than the optimal size (the dotted line shows the division between the 2 groups in Fig. 10). Although such a division is somewhat arbitrary, reducing spot sizes into the two groups allowed us to address the question easily. Furthermore, results obtained from different cells could be easily combined by "normalizing" spot sizes with respect to the receptive field center diameter.

Figure 11*A* shows the responses of the same cell as in Fig. 10 before, during, and after 86 nA of D-APV application. Although D-APV decreased the background activity and the responses at all spot sizes, the extent of the decrease was greater for the center responses than for the center + surround responses. To compare the effect of D-APV on the visual response alone, the background response (either before or during D-APV application) was subtracted from each of the responses (Fig. 11*B*). The two center responses (at 1.2 and 2.4 deg) decreased significantly (by 92 and 71%, respectively), whereas one of the center + surround responses (at 4.8 deg) decreased only slightly (by 33%) and the other (at 9.6 deg) actually increased (by 92%) with D-APV (Fig. 11*C*). This differential effect of D-APV is especially clear if one compares the responses at 1.2 and 9.6 deg. Even though the control responses at the two sizes were similar, D-APV decreased the former but increased the latter. Proportional reductions were computed for each of the two groups by combining the two center responses (at 1.2

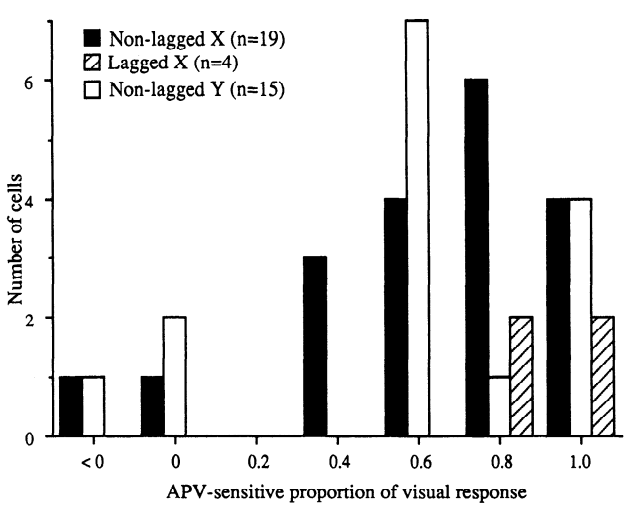

FIG. 7. Frequency distribution histogram of the D-2-amino-5-phosphonovaleric acid (D-APV)-sensitive fractions (derived from the contrast study) among different cell types. Mean for lagged X cells: 0.896 ± 0.065, $n = 4$; nonlagged X cells: 0.636 ± 0.070, $n = 19$; nonlagged Y cells: 0.567 ± 0.100, $n = 15$.

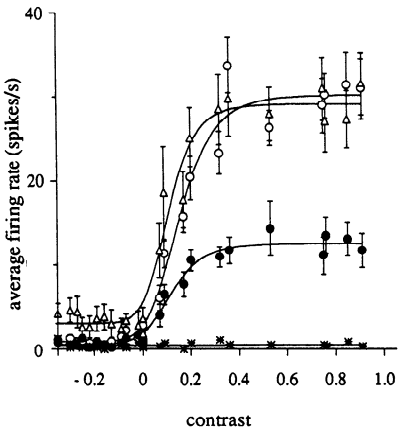

FIG. 8. Contrast-response curves of an off-center nonlagged X cell (same cell as in Fig. 6*A*) before (○), during 86 nA of D-2-amino-5-phosphonovaleric acid (D-APV) iontophoresis (●), during simultaneous application of 86 nA of D-APV and 83 nA of 6-cyano-7-nitroquinoxaline-2,3-dione (CNQX, ⋆), and 2 min after iontophoresis (△). Note the significant decrease in the gain of the contrast-response curve by D-APV and complete abolition of visual responses with the additional application of CNQX.

and 2.4 deg) as well as the two center + surround responses (4.8 and 9.6 deg) together; the sum of the reductions by D-APV was divided by the sum of the control responses in each of the two groups. Figure 11 *D* shows that the D-APV-sensitive fraction of the center responses was substantially greater than that of the center + surround responses (0.76 and −0.04, respectively).

Different levels of contribution of NMDA receptors to the two groups of responses were evident in all cell classes. Figure 12 shows results from four different cell types. In each case, the D-APV-sensitive proportion was greater for the center than for the center + surround responses. Figure 12, *A* and *B*, shows an off-center nonlagged X cell whose D-APV-sensitive fractions of the center and center + surround responses were 0.70 and −0.23, respectively. Figure 12, *C* and *D*, shows an on-center nonlagged X cell whose D-APV-sensitive fractions of the center and center + surround responses were 1.00 and 0.52, respectively. Figure 12, *E* and *F*, shows an off-center lagged X cell whose D-APV-sensitive fractions were 1.00 and 0.64, whereas *G* and *H* show an on-center nonlagged Y cell whose D-APV-sensitive fractions were 0.80 and 0.41. Figure 12 shows that neither the particular optimal spot size nor the particular value of the D-APV-sensitive fraction for a given cell affect the fact that increased (intrageniculate) surround inhibition (via larger spots) decreased the proportional contribution of NMDA receptors to the visual response.

For each cell tested, we calculated the difference between the D-APV-sensitive fractions of the center and center + surround responses (center minus center + surround). The results are shown in the frequency distribution histogram of Fig. 13. The 0 column contains cells for which the D-APV-sensitive fraction of the center responses was within ±0.05 of the center + surround responses. The positive columns show cells in which the D-APV-sensitive fraction of the center responses was greater than that of the center +

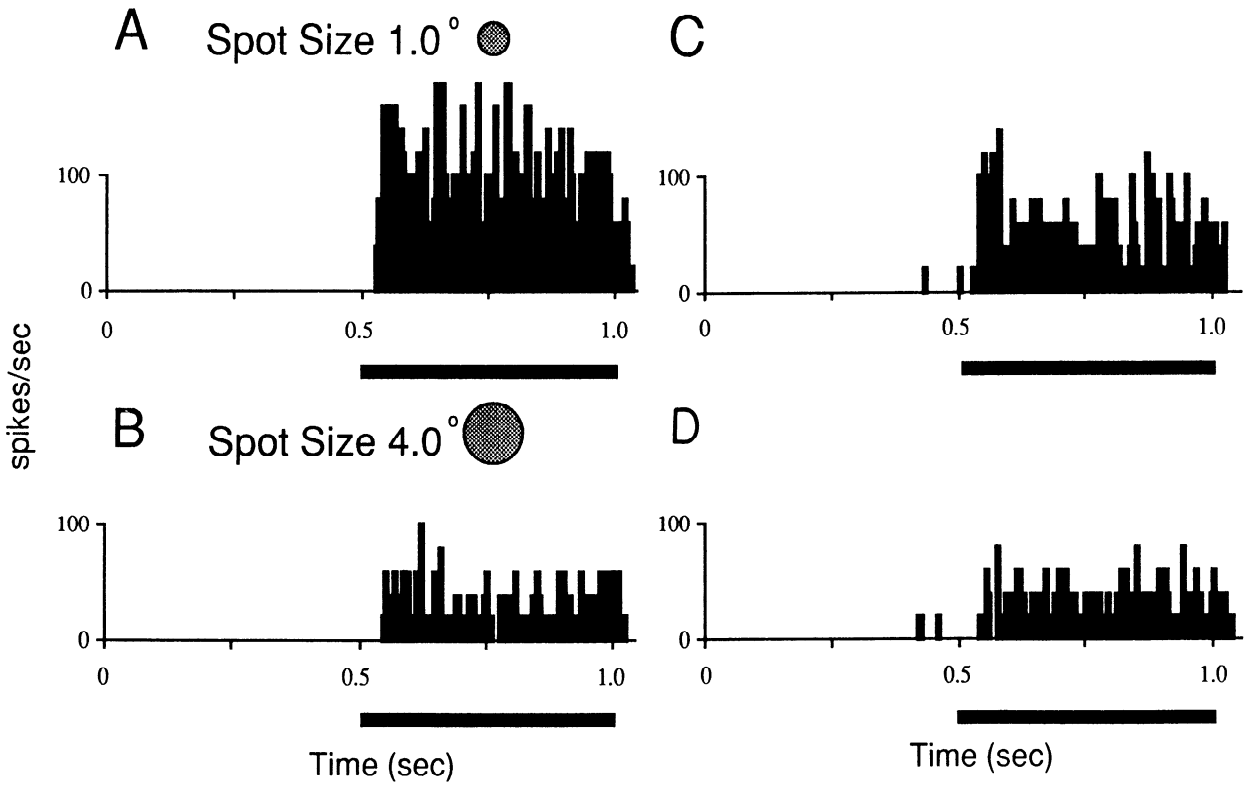

FIG. 9. Responses of an off-center X cell to spots of varying sizes and the effect of D-2-amino-5-phosphonovaleric acid (D-APV). Each histogram represents summed responses to 10 presentations of a dark spot of contrast 0.9. Each bin spans 5 ms. Timing and duration of the visual stimulus is indicated by the bar below each histogram. *A*: control (predrug) response to an spot of optimal size (matched to the receptive field center). *B*: control response to a large spot. *C* and *D*: responses during iontophoretic application of D-APV (86 nA). Note that although there is a clear reduction in response to the optimally sized spot, there is little change in the response to a larger spot.

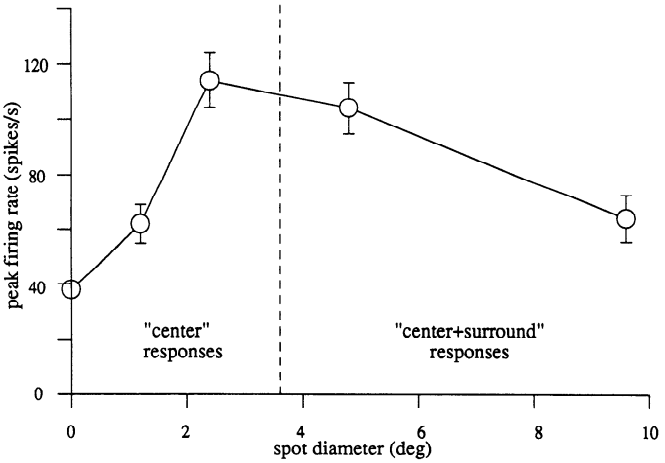

FIG. 10. Size-response plot for an off-center nonlagged X cell. Error bars: SE of the peak firing rate averaged over 10 trials. Dotted line: division between center and center + surround responses.

surround responses. The negative columns represent cells in which the reverse was true. The data show that, although cells vary widely in the relative D-APV-sensitivity of their center and center + surround responses, the distribution is biased in favor of cells showing greater D-APV-sensitivity for center responses. The mean D-APV-sensitive proportion of the center responses was 0.581 ± 0.053 (n = 34), and that of the center + surround responses was 0.353 ± 0.106 (n = 34). The mean of the individual differences between the two was 0.228 ± 0.085 (marked by triangle in Fig. 13), and this difference was statistically significant ($P < 0.02$, Wilcoxon signed-rank test). These results suggest that intrageniculate inhibition induced by stimulating larger regions of retina (and dLGN) reduces the activation of NMDA receptors mediating the visual responses of dLGN neurons.

Comparison between responses evoked by varying contrast and spot sizes

The contrast-response functions before and after D-APV application, and hence the contribution of NMDA receptors to the visual response at different contrasts, were obtained with the spot size fixed at optimal. The size-response functions, on the other hand, were obtained with different-sized spots at a fixed contrast. However, given the linear relationship between the D-APV-sensitive fraction and control visual response at different contrasts (Figs. 2, 3, and 5), the fraction obtained from the first study should match closely the center responses obtained from the second study. We wished to establish if this were true for individual cells. We also wished to compare the fraction obtained from the first study with the fraction from the center + surround responses obtained from the second study.

Figure 14*A* shows the frequency distribution histogram of the difference in the D-APV-sensitive fraction between the value obtained by varying contrast at optimal spot size and the value for center responses (for the same cell) obtained by varying spot sizes at a fixed contrast. The positive columns indicate cells whose D-APV-sensitive proportion was greater for the optimal spot than for the center spots. The difference in the D-APV-sensitive fractions was not statistically significant (mean of the individual differences = 0.073 ± 0.050, represented by the triangle in Fig. 14*A*; $P > 0.2$, Wilcoxon signed-rank test). On the other hand, the difference between the D-APV-sensitive fraction at optimal spot size and center + surround responses (0.288 ± 0.113, marked by triangle in Fig. 14*B*) was statistically significant (P = 0.02; mean for optimal spots 0.634 ± 0.053; mean for center + surround, 0.346 ± 0.113; n = 32). Thus the D-APV-sensitive fraction is smaller with surround inhibition than with center stimulation alone, whether the center was driven with varying contrasts at a

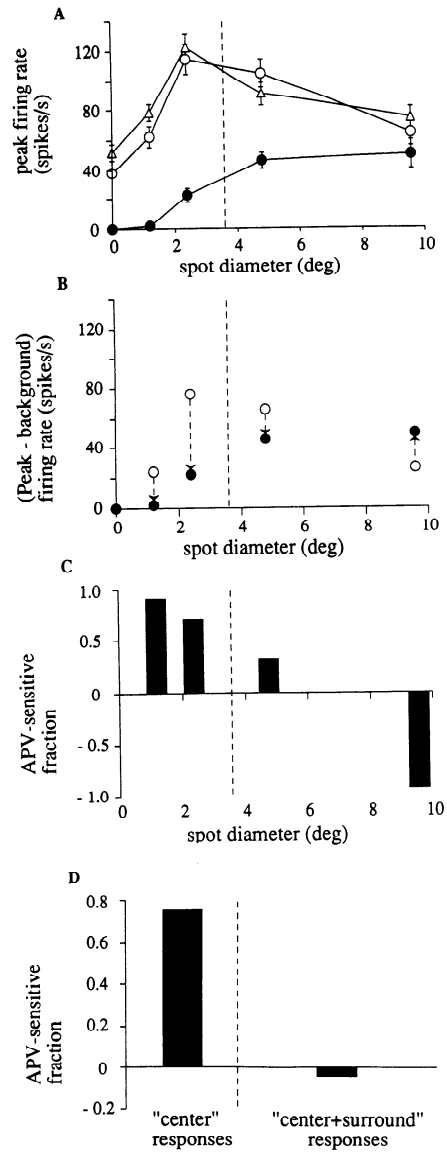

FIG. 11. Effect of D-2-amino-5-phosphonovaleric acid (D-APV) on the size-response plot of the cell in Fig. 10. *A*: size-response plot before (○), during (●), and after (△) 86 nA of D-APV application. Conventions as in Fig. 10. *B*: same plot with only the predrug control and D-APV responses, each with their respective background firing rate subtracted. Arrows: direction and magnitude of the D-APV effect for each of the 4 responses. *C*: histogram of the D-APV-sensitive component as a fraction of the control responses at each spot size. Note that there is an inverse relationship between the D-APV-sensitive fraction and spot size. *D*: histogram of the D-APV-sensitive component as proportions of the control for center and center + surround responses. The D-APV-sensitive fraction was greater for the center responses than for the center + surround responses.

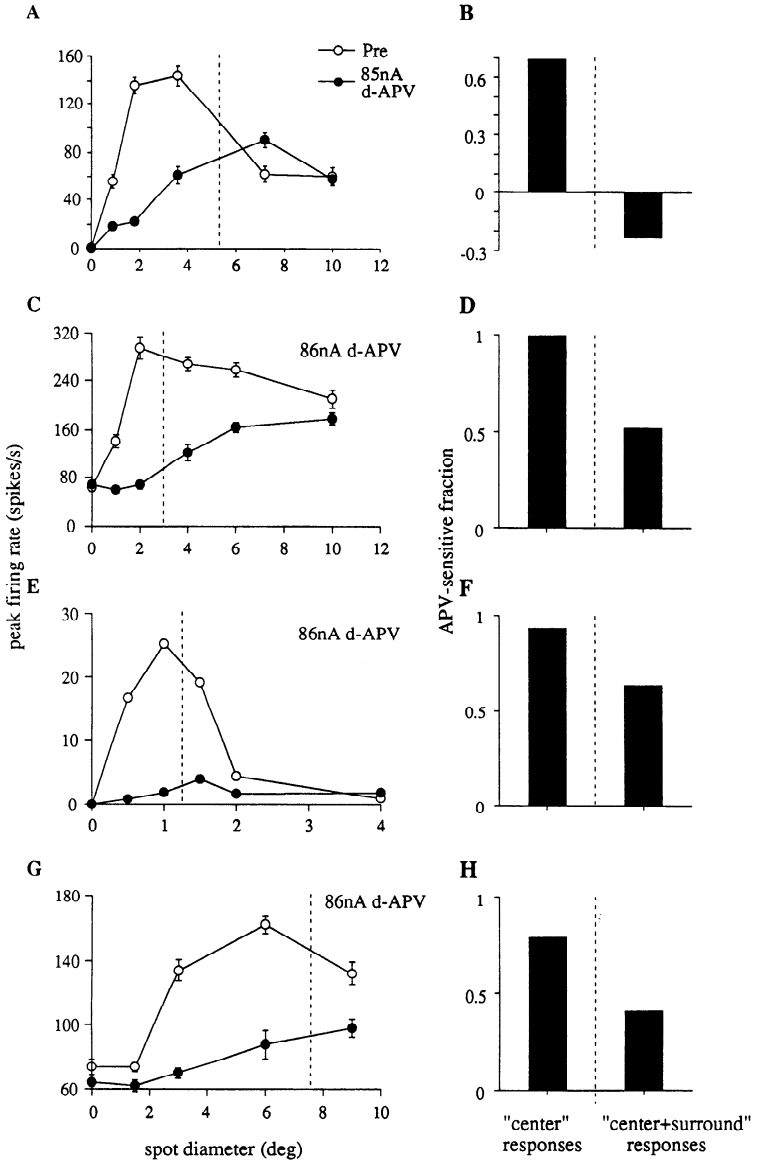

FIG. 12. Effect of D-2-amino-5-phosphonovaleric acid (D-APV) on size-response plots of 4 different dorsal lateral geniculate nucleus (dLGN) cells. *A*: off-center nonlagged X cell before and during application of 85 nA of D-APV. *B*: same cell as in *A*. Histogram of D-APV-sensitive fraction of the center and center + surround responses. *C* and *D*: on-center nonlagged X cell before and during application of 86 nA of D-APV. Histogram convention same as *B*. *E* and *F*: off-center lagged X cell before and during application of 86 nA of D-APV. *G* and *H*: on-center nonlagged Y cell before and during application of 86 nA of D-APV. In all 4 cells, the D-APV-sensitive fraction is greater for the center responses than for the center + surround responses.

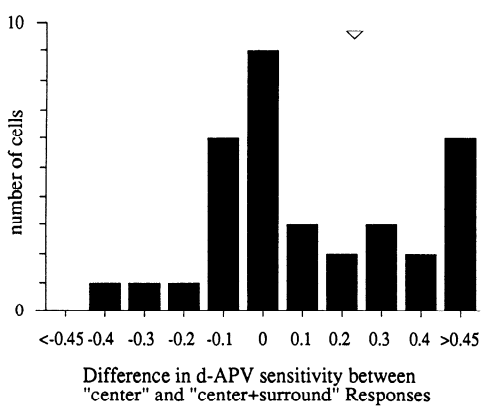

FIG. 13. Frequency distribution histogram of the difference in the D-2-amino-5-phosphonovaleric acid (D-APV)-sensitive fraction between the center and center + surround responses (n = 34 cells). The actual values are computed by subtracting the D-APV-sensitive fraction of the center + surround responses from that of the center responses. Thus positive columns represent bigger D-APV sensitive fractions for the center responses, and the negative columns represent the reverse. Open triangle: mean difference.

fixed optimal spot size or by varying sizes (up to and including the optimal size) at a fixed contrast.

In summary, these results suggest that different levels of retinal excitatory drive activate a constant proportion of NMDA receptors on dLGN neurons and therefore do not modulate NMDA receptor activation, at least when monitored extracellularly. However, increasing the spatial extent of intrageniculate inhibition does reduce the proportion of the visual response mediated by NMDA receptors. That is, altering the balance of excitation and inhibition on dLGN neurons via intrageniculate inhibition can modulate the level of NMDA receptor activation.

DISCUSSION

There are three main results of the present study. First, NMDA receptors contribute to visual responses of dLGN cells, and their effect is prominent both in the linear range of the contrast-response curve and in the saturation response. Second, the magnitude of the D-APV-sensitive

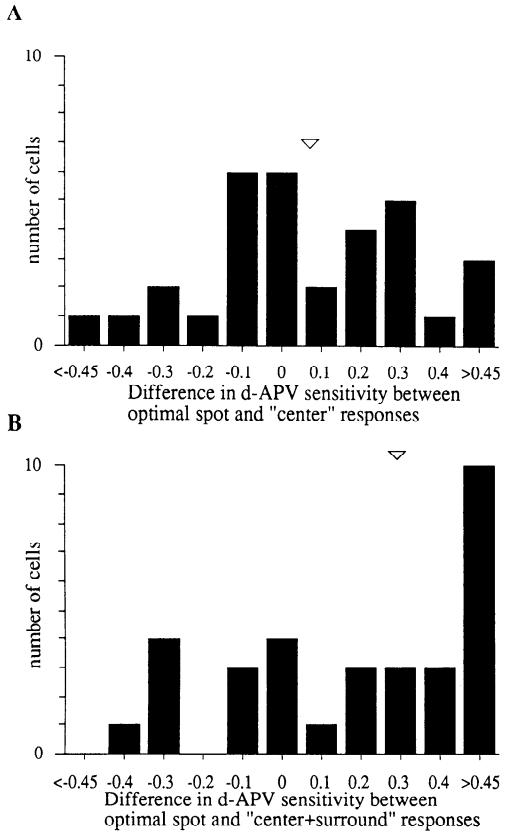

FIG. 14. Frequency distribution histogram of the differences between the D-2-amino-5-phosphonovaleric acid (D-APV)-sensitive fraction obtained with the use of an optimal spot size at different contrasts and that of (*A*) center response and (*B*) center + surround response. Conventions as in Fig. 13.

component of the visual response is a linear function of the control visual response level. Third, the D-APV-sensitive component of the visual response decreases with increasing surround inhibition.

Contribution of NMDA receptors to visual responses

Blockade of NMDA receptors reduced the slope and the amplitude of the saturation response of the contrast-response curve. It did not, however, significantly change the threshold contrast, saturation contrast, or C_{50}. These results are similar to those obtained in a recent report on the role of NMDA receptors in the superficial layers of the cat's visual cortex (Fox et al. 1990). To directly assess the magnitude of the NMDA receptor component at varying levels of visual responses, we plotted the D-APV-sensitive component as a function of control response (Figs. 2, 3, and 5). This showed clearly that, for most cells, the NMDA receptor component is a linear function of the visual response amplitude. Thus D-APV reduced the smallest responses (near threshold contrast) just as much as it did the responses near saturation. It is worth noting that we presented stimulus contrasts covering nearly all of the range over which LGN neurons can transmit meaningful information about retinal contrast to the visual cortex. Our results suggest that the nonlinear voltage dependence of the NMDA receptor reported in recent in vitro studies of the LGN (Esguerra et al. 1992) does not appear to play a significant role in the encoding of stimulus contrast by LGN neurons.

Previous studies of hippocampus (Herron et al. 1986) or ventrobasal thalamus (Salt 1986; however, see also Salt and Eaton 1991) neurons have suggested that only high-frequency inputs can activate NMDA receptors. In these studies, low-frequency stimulation was apparently not sufficient to overcome the Mg^{2+} block of NMDA receptors. On the basis of these studies, one might have predicted that NMDA receptor activation would be a nonlinear function of retinal input; specifically, one would predict little or no activation of NMDA receptors at low levels of excitatory input (and therefore low response levels) and proportionally greater activation at high levels of input (high response levels). This was not observed in the present study. The proportion of NMDA receptors involved in the visual response remained similar over a wide range of contrasts. The mechanistic implication is that at threshold contrast (i.e., contrast sufficient to evoke a measureable increase in firing rate) LGN neurons are sufficiently depolarized so as to remove the Mg^{2+} block of their NMDA receptors.

There are several possible explanations for the apparent differences between dLGN neurons and neurons in systems that have shown the necessity of high-frequency stimulation for NMDA receptor activation. First, the visual responses that we measured extracellularly in the dLGN are driven by afferent retinal ganglion cells with background firing rates of 40–50 Hz (Kaplan et al. 1987). In addition, retinogeniculate afferent input is likely to be sustained in many cells for as long as the visual stimulus persists (0.5 s in our experiments). These more natural stimulus conditions are very different from the single electrical shocks delivered to afferent fibers that were used in the other studies. Tonic afferent inputs of 40–50 Hz are likely to provide sufficient postsynaptic depolarization to overcome the voltage-dependent Mg^{2+} block of the NMDA receptor. Second, dLGN cells in vivo receive input not only from retinal afferents but also from a variety of nonretinal sources (for review, see Sherman and Koch 1986). These inputs may serve to maintain the membrane potential of dLGN neurons at more depolarized levels than neurons in other systems. Third, ambient levels of glutamate (Sah et al. 1989) may tonically activate EAA receptors on dLGN neurons. Indeed, even a single electrical shock to the optic tract has been found to be sufficient to activate NMDA receptors that contribute to excitatory postsynaptic potentials (EPSPs) in the LGN in vitro (Esguerra and Sur 1990; Esguerra et al. 1992; Scharfman et al. 1990), and single electrical stimuli can activate NMDA receptors in the ventrobasal thalamus of the rat as well (Salt and Eaton 1991).

NMDA component of the visual response in different cell classes

When we compared the proportion of the visual response due to NMDA receptors among different physiological classes of cells in the dLGN, we found that NMDA receptors contributed more to the responses of lagged X cells than nonlagged X or Y cells (we recorded no lagged Y cells in this study). This result is consistent with those of previous studies (Heggelund and Hartveit 1990; Kwon et al. 1991). The present results show that the difference in the proportional contribution of NMDA receptors between cell

classes, and indeed between different cells, cannot be due to differences in visual response levels. This is also consistent with results from our previous study in which we found no correlation between the average level of predrug visual activity and the effect of D-APV on visual responses of lagged or nonlagged cells (Kwon et al. 1991).

Interaction of intrageniculate inhibition and NMDA receptor-mediated excitation

γ-aminobutyric acid (GABA)ergic inhibition is known to play a significant role in the processing of retinal signals in the dLGN (Berardi and Morrone 1984; Sillito and Kemp 1983; for review, see Sherman and Koch 1986). Local application of bicuculline in the dLGN reduces the strength of surround inhibition (Sillito and Kemp 1983). We used the fact that large stimuli generate increased lateral intrageniculate inhibition to study the effect of that inhibition on D-APV sensitivity. We found that responses to large stimuli were reduced less by D-APV than were responses to small stimuli. One interpretation of these results is that NMDA receptor activation decreases with increasing intrageniculate inhibition. Intracellular studies in vivo and in vitro suggest some possible synaptic mechanisms by which this could occur. In vivo, inhibitory postsynaptic potentials (IPSPs) in LGN relay neurons are of three types: short, medium, and long duration (Bloomfield and Sherman 1988). On the basis of reversal potential, the short-duration IPSPs are believed to be mediated by $GABA_A$ receptors and the medium- and long-duration IPSPs by $GABA_B$ receptors. In vitro studies have confirmed the presence of two pharmacologically distinct IPSPs in LGN neurons, a short-lasting (3- to 5-ms) IPSP mediated by $GABA_A$ receptors and a delayed (20- to 40-ms) long-lasting IPSP mediated by $GABA_B$ receptors (Crunelli et al. 1988; Hirsch and Burnod 1987; Soltesz et al. 1989; for review, see Crunelli and Leresche 1991). Both types of IPSPs can be elicited by optic tract stimulation in an LGN slice preparation that does not contain the perigeniculate nucleus, a potential source of inhibitory input to LGN relay cells. This leaves the intrinsic interneurons in the LGN as the source of the two IPSP types. The $GABA_A$ receptor–mediated IPSP produces a shunting inhibition through Cl^- channels, and the $GABA_B$ receptor produces hyperpolarization through K^+ channels.

Optic tract evoked EPSPs recorded in the LGN reveal NMDA receptor–mediated components that are relatively sustained (Esguerra et al. 1992; Scharfman et al. 1990). Similar results have been found in the ventrobasal thalamus (Salt and Eaton 1991) and visual cortex (Jones and Baughman 1988). Taken together with what we know of the two types of GABAergic inhibition in the dLGN, it seems not unlikely that the long-lasting $GABA_B$ receptor–mediated IPSP may be able to selectively reduce the sustained component of the EPSPs mediated by NMDA receptors in the dLGN. Furthermore, $GABA_B$ receptor–mediated hyperpolarization can lead to Mg^{2+} block of NMDA receptors while actually increasing non-NMDA responses by increasing driving force. Indeed, such $GABA_B$-mediated inhibition of the NMDA component of synaptic potentials has recently been reported in the hippocampus (Morrisett et al. 1991). However, in the visual cortex, it has been also shown that NMDA receptor activation is blocked by $GABA_A$ receptor–mediated inhibition (Artola and Singer 1987).

An alternative explanation for the observed difference between center and center + surround responses is that iontophoretic application of D-APV reduces excitation to relay cells as well as to intrageniculate interneurons, thus altering the balance of excitation and inhibition on relay cells. A paradoxical increase in response with NMDA blockade in the dLGN has been recently reported for some cells by Hartveit and Heggelund (1990). In a few cells recorded in slices of the LGN in vitro, optic tract evoked IPSPs (as well as the EPSPs) decrease with application of D-APV in dLGN slices (M. Esguerra, Y. H. Kwon, and M. Sur, unpublished results). In the present study, we did observe several cells that increased their spontaneous firing rate with the application of D-APV (data not shown), and in some cases the response to the largest spot (presumably leading to the greatest amount of intrageniculate inhibition) was increased by D-APV (Fig. 12). Most cells, however, did not show increases in spontaneous firing suggestive of disinhibition, and a significant number of cells in fact showed reduced spontaneous firing.

Our results with large spots suggest that one possible reason why the fraction of the visual response mediated by NMDA receptors varies between cells is difference in the amount of inhibition on cells. However, we found different NMDA-mediated proportions when we used spots of optimal size that elicited little or no surround inhibition. It is also possible that the variable contribution of NMDA receptors results from technical aspects of microiontophoresis (e.g., distance of the iontophoretic barrel from dendrites, differences between cells in rates of diffusion, rates of uptake, etc.). We consider this unlikely for two reasons. First, we were careful to wait a period of time (>2 min) after the start of iontophoresis to allow drugs to reach a "steady-state" concentration around the cell from which we were recording. Second, optic tract evoked EPSPs in LGN neurons in a slice preparation also differ in their D-APV sensitivity even under the same concentration of D-APV (Esguerra et al. 1992). Therefore the variability in the NMDA component of the visual response among different cells and cell classes is likely to be a reflection of different amounts of NMDA receptors that are either present on these cells or that are recruited for the visual response.

It is useful here to distinguish between two possible kinds of intrageniculate inhibition: feedforward inhibition and lateral inhibition (Fig. 15). It is reasonable to postulate that feedforward inhibition arises from the same afferents that provide the major excitatory drive to a relay cell. Feedforward inhibition would increase as the excitatory drive from retinal afferents increases (such as with increasing stimulus contrast). However, the balance of excitation and inhibition would remain the same at different levels of contrast. Lateral inhibition arises from afferents that are spatially separate from those that provide the major excitatory drive to a relay cell; lateral inhibition would increase as stimulus size increases to include greater retinal area. Thus the balance of excitation and inhibition would change as spot size is varied. Our results suggest strongly that the proportional contribution of NMDA receptors to dLGN cell responses

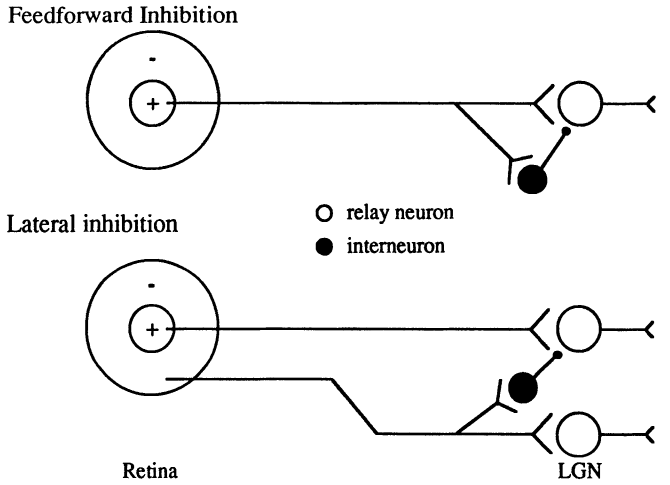

FIG. 15. Two different kinds of inhibition on dorsal lateral geniculate nucleus (dLGN) relay cells, and their spatial relationship to the center (+) and surround (−) of a dLGN cell receptive field. The results of this study suggest that varying feedforward inhibition does not alter the proportional contribution of *N*-methyl-D-aspartate (NMDA) receptors to the visual responses of dLGN cells, whereas varying lateral inhibition does.

can be modulated by lateral inhibition but not by feedforward inhibition. Consistent with this view, we find that lagged cells, which are thought to receive greater feedforward inhibition (Humphrey and Weller 1988b; Mastronarde 1987b), are actually more sensitive to NMDA receptor blockade. Our data do not provide a definitive answer to the question of why feedforward and lateral inhibition should have different effects on NMDA receptor–mediated responses. Presumably, the IPSPs evoked by lateral inhibitory circuits are more effective in producing hyperpolarization of the dendritic regions where synaptic NMDA receptors are located. Such a difference between lateral and feedforward IPSPs could be due to differences in inhibitory receptor subtype, in IPSP time course, or in the spatial location of inhibitory inputs.

Role of NMDA receptors in the dLGN

In vitro, NMDA receptors on dLGN cells can mediate nonlinear transfer of retinal input to cortex (Esguerra et al. 1992). The nonlinear nature of NMDA receptor activation has been hypothesized to underlie the gating of retinogeniculate transmission by corticofugal input to the dLGN (Koch 1987), and this possibility has recently been demonstrated in vitro (Esguerra and Sur 1990). In the present study, we investigated the relationship between NMDA receptor activation and two visual stimulus parameters: contrast and size. We found that the response attributable to NMDA receptor activation increased linearly with contrast but was a nonlinear function of stimulus size. Our interpretation of these findings is that NMDA receptors are not modulated by changes in retinal excitatory drive, but are modulated by lateral inhibitory inputs. This implies that NMDA receptors provide an additional mechanism by which inhibitory inputs can affect the transmission of retinal information to the cortex. Inhibitory interneurons in turn receive inputs from a variety of sources, including retinal, corticofugal (Weber et al. 1989), and cholinergic brain stem (Ahlsén et al. 1984; Singer 1973; Singer and Dräger 1972) afferents. NMDA receptors may therefore allow changes in inhibition that accompany changes in the visual stimulus or in the behavioral state of the animal to modulate excitatory synaptic transmission through the LGN.

We thank M. Esguerra and A. Roe for general advice and comments and A. Passera and R. Dolan for technical advice on data analysis programs.

This work was supported by Grant EY 07023 from the National Eye Institute.

Address for reprint requests: M. Sur, Dept. of Brain and Cognitive Sciences, M.I.T., E25-618, Cambridge, MA 02139.

Received 5 June 1991; accepted in final form 18 February 1992.

REFERENCES

AHLSÉN, G., LINDSTRÖM, S., AND LO, F.-S. Inhibition from the brain stem of inhibitory interneurons of the cat's dorsal lateral geniculate nucleus. *J. Physiol. Lond.* 347: 593–609, 1984.

ARTOLA, A. AND SINGER, W. Long-term potentiation and NMDA receptors in rat visual cortex. *Nature Lond.* 330: 649–652, 1987.

BERARDI, N. AND MORRONE, M. C. The role of γ-aminobutyric acid mediated inhibition in the response properties of cat lateral geniculate nucleus neurones. *J. Physiol. Lond.* 357: 505–523, 1984.

BLOOMFIELD, S. A. AND SHERMAN, S. M. Postsynaptic potentials recorded in neurons of the cat's lateral geniculate nucleus following electrical stimulation of the optic chiasm. *J. Neurophysiol.* 60: 1924–1945, 1988.

COTMAN, C. W., MONAGHAN, D. T., OTTERSEN, O. P., AND STORM-MATHISEN, J. Anatomical organization of excitatory amino acid receptors and their pathways. *Trends Neurosci.* 10: 273–280, 1987.

CRUNELLI, V., HABY, M., JASSIK-GERSCHENFELD, D., LERESCHE, N., AND PIRCHIO, M. Cl^- and K^+-dependent inhibitory postsynaptic potentials evoked by interneurones of the rat lateral geniculate nucleus. *J. Physiol. Lond.* 399: 153–176, 1988.

CRUNELLI, V., KELLY, J. S., LERESCHE, N., AND PIRCHIO, M. On the excitatory post-synaptic potential evoked by stimulation of the optic tract in the rat lateral geniculate nucleus. *J. Physiol. Lond.* 384: 603–618, 1987.

CRUNELLI, V. AND LERESCHE, N. A role for $GABA_B$ receptors in excitation and inhibition of thalamocortical cells. *Trends Neurosci.* 14: 16–21, 1991.

ESGUERRA, M., KWON, Y. H., AND SUR, M. Retinogeniculate EPSPs recorded intracellularly in the ferret lateral geniculate nucleus in vitro: role of NMDA receptors. *Visual Neurosci.* 8: 545–555, 1992.

ESGUERRA, M. AND SUR, M. Corticogeniculate feedback gates retinogeniculate transmission by activating NMDA receptors. *Soc. Neurosci. Abstr.* 16: 159, 1990.

FOX, K., SATO, H., AND DAW, N. The effect of varying stimulus intensity on NMDA-receptor activity in cat visual cortex. *J. Neurophysiol.* 64: 1413–1428, 1990.

FUNKE, K., EYSEL, U. T., AND FITZGIBBON, T. Retinogeniculate transmission by NMDA and non-NMDA receptors in the cat. *Brain Res.* 547: 229–238, 1991.

GILBERTSON, T. A., SCOBEY, R., AND WILSON, M. Permeation of calcium ions through non-NMDA glutamate channels in retinal bipolar cells. *Science Wash. DC* 251: 1613–1615, 1991.

HARTVEIT, E. AND HEGGELUND, P. Neurotransmitter receptors mediating excitatory input to cells in the cat lateral geniculate nucleus. II. Nonlagged cells. *J. Neurophysiol.* 63: 1361–1372, 1990.

HEGGELUND, P. AND HARTVEIT, E. Neurotransmitter receptors mediating excitatory input to cells in the cat lateral geniculate nucleus. I. Lagged cells. *J. Neurophysiol.* 63: 1347–1360, 1990.

HERRON, C. E., LESTER, R. A. J., COAN, E. J., AND COOLINGRIDGE, G. L. Frequency-dependent involvement of NMDA receptors in the hippocampus: a novel synaptic mechanism. *Nature Lond.* 322: 265–267, 1986.

HIRSCH, J. C. AND BURNOD, Y. Synaptically evoked late hyperpolarization in the rat dorsolateral geniculate neurons in vitro. *Neuroscience* 23: 457–468, 1987.

HUBEL, D. H. AND WIESEL, T. N. Integrative action in the cat's lateral geniculate body. *J. Physiol. Lond.* 155: 385–398, 1961.

HUMPHREY, A. L. AND WELLER, R. E. Functionally distinct groups of X-cells in the lateral geniculate nucleus of the cat. *J. Comp. Neurol.* 268: 429–447, 1988a.

HUMPHREY, A. L. AND WELLER, R. E. Structural correlates of functionally distinct X-cells in the lateral geniculate nucleus of the cat. *J. Comp. Neurol.* 268: 448–468, 1988b.

JONES, K. A. AND BAUGHMAN, R. W. NMDA- and non-NMDA-receptor components of excitatory synaptic potentials recorded from cells in layer V of rat visual cortex. *J. Neurosci.* 8: 3522–3534, 1988.

KAPLAN, E., PURPURA, K., AND SHAPLEY, R. M. Contrast affects the transmission of visual information through the mammalian lateral geniculate nucleus. *J. Physiol. Lond.* 391: 267–288, 1987.

KEMP, J. A. AND SILLITO, A. M. The nature of the excitatory transmitter mediating X and Y cell inputs to the cat dorsal lateral geniculate nucleus. *J. Physiol. Lond.* 323: 377–391, 1982.

KOCH, C. The action of the corticofugal pathway on sensory thalamic nuclei: a hypothesis. *Neuroscience* 23: 399–406, 1987.

KWON, Y. H., ESGUERRA, M., AND SUR, M. NMDA and non-NMDA receptors mediate visual responses of neurons in the cat's lateral geniculate nucleus. *J. Neurophysiol.* 66: 414–428, 1991.

MASTRONARDE, D. N. Two classes of single-input X-cells in cat lateral geniculate nucleus. I. Receptive-field properties and classification of cells. *J. Neurophysiol.* 57: 357–380, 1987a.

MASTRONARDE, D. N. Two classes of single-input X-cells in cat lateral geniculate nucleus. II. Retinal inputs and the generation of receptive-field properties. *J. Neurophysiol.* 57: 381–413, 1987b.

MASTRONARDE, D. N. Branching of X and Y functional pathways in cat lateral geniculate nucleus. *Soc. Neurosci. Abstr.* 14: 309, 1988.

MAYER, M. L. AND WESTBROOK, G. L. The physiology of excitatory amino acids in the vertebrate central nervous system. *Prog. Neurobiol.* 28: 197–276, 1987.

MACDERMOTT, A. B. AND DALE, N. Receptors, ion channels and synaptic potentials underlying the integrative actions of excitatory amino acids. *Trends Neurosci.* 10: 280–284, 1987.

MORRISETT, R. A., MOTT, D. D., LEWIS, D. V., SWARTZWELDER, H. S., AND WILSON, W. A. $GABA_B$-receptor–mediated inhibition of the *N*-methyl-D-aspartate component of synaptic transmission in the reat hippocampus. *J. Neurosci.* 11: 203–209, 1991.

SAH, P., HESTRIN, S., AND NICOLL, R. A. Tonic activation of NMDA receptors by ambient glutamate enhances excitability of neurons. *Science Wash. DC* 246: 815–818, 1989.

SALT, T. E. Mediation of thalamic sensory input by both NMDA receptors and non-NMDA receptors. *Nature Lond.* 322: 263–265, 1986.

SALT, T. E. AND EATON, S. A. Sensory excitatory postsynaptic potentials mediated by NMDA and non-NMDA receptors in the thalamus in vivo. *Eur. J. Neurosci.* 3: 296–300, 1991.

SAUL, A. AND HUMPHREY, A. L. Spatial and temporal response properties of lagged and non-lagged cells in the cat lateral geniculate nucleus. *J. Neurophysiol.* 64: 206–224, 1990.

SCHARFMAN, H. E., LU, S.-M., GUIDO, W., ADAMS, P. R., AND SHERMAN, S. M. *N*-methyl-D-aspartate receptors contribute to excitatory postsynaptic potentials of cat lateral geniculate neurons recorded in thalamic slices. *Proc. Natl. Acad. Sci. USA.* 87: 4548–4552, 1990.

SHAPLEY, R. AND LENNIE, P. Spatial frequency analysis in the visual system. *Annu. Rev. Neurosci.* 8: 547–583, 1985.

SHERMAN, S. M. AND KOCH, C. The control of retinogeniculate transmission in the mammalian lateral geniculate nucleus. *Exp. Brain Res.* 63: 1–20, 1986.

SHERMAN, S. M. AND SPEAR, P. D. Organization of visual pathways in normal and visually deprived cats. *Physiol. Rev.* 62: 738–855, 1982.

SILLITO, A. M. AND KEMP, J. A. The influence of GABAergic inhibitory processes on the receptive field structure of X and Y cells in cat dorsal lateral geniculate nucleus (dLGN). *Brain Res.* 277: 63–77, 1983.

SILLITO, A. M., MURPHY, P. C., AND SALT, T. E. The contribution of the non-*N*-methyl-D-aspartate group of excitatory amino acid receptors to retinogeniculate transmission in the cat. *Neuroscience* 34: 273–280, 1990a.

SILLITO, A. M., MURPHY, P. C., SALT, T. E., AND MOODY, C. I. Dependence of retinogeniculate transmission in cat on NMDA receptors. *J. Neurophysiol.* 63: 347–355, 1990b.

SINGER, W. The effect of mesencephalic reticular stimulation on intracellular potentials of cat lateral geniculate neurons. *Brain Res.* 61: 35–54, 1973.

SINGER, W. AND DRÄGER, U. Postsynaptic potentials in relay neurons of cat lateral geniculate nucleus after stimulation of the mesencephalic reticular formation. *Brain Res.* 41: 214–220, 1972.

SOLTESZ, I., LIGHTOWLER, S., LERESCHE, N., AND CRUNELLI, V. On the properties and origin of the $GABA_B$ inhibitory postsynaptic potential recorded in morphologically identified projection cells of the cat dorsal lateral geniculate nucleus. *Neuroscience* 33: 23–33, 1989.

SUR, M., ESGUERRA, M., GARRAGHTY, P. E., KRITZER, M. F., AND SHERMAN, S. M. Morphology of physiologically identified retinogeniculate X- and Y-axons in the cat. *J. Neurophysiol.* 52: 1–32, 1987.

UHLRICH, D. J., TAMAMAKI, N., AND SHERMAN, S. M. Brainstem control of response modes in neurons of the cat's lateral geniculate nucleus. *Proc. Natl. Acad. Sci. USA* 87: 2560–2563, 1990.

WEBER, A. J., KALIL, R. E., AND BEHAN, M. Synaptic connections between corticogeniculate axons and interneurons in the dorsal lateral geniculate nucleus of the cat. *J. Comp. Neurol.* 289: 156–164, 1989.